Motorized and Functional Electrical Stimulation Induced Cycling via Switched Repetitive Learning Control

Victor H. Duenas[ID], Christian A. Cousin[ID], Anup Parikh[ID], Paul Freeborn,
Emily J. Fox, and Warren E. Dixon, *Fellow, IEEE*

Abstract—Cycling induced by functional electrical stimulation (FES) coupled with motorized assistance is a promising rehabilitative strategy. A switching controller that activates lower limb muscles alongside an electric motor based on the crank angle is developed to facilitate cycling. Due to the periodic nature of cadence tracking in cycling, a repetitive learning controller (RLC) is developed to track a desired cadence trajectory with a known period. The RLC is developed for an uncertain, nonlinear cycle-rider system with autonomous state-dependent switching. Electrical stimulation switches across multiple lower limb muscle groups based on the torque effectiveness throughout the crank cycle. The electric motor provides assistance when the muscle groups yield low torque production. A Lyapunov-based stability analysis that invokes a recently developed LaSalle–Yoshizawa corollary for nonsmooth systems is used to guarantee asymptotic tracking. The developed controller was tested during FES-cycling experiments in five able-bodied individuals and three participants with neurological conditions. The added value of the RLC in cadence tracking is illustrated by comparing the results of two trials with and without the learning feedforward term. The results indicate that the RLC yields a lower mean root-mean-squared cadence tracking error.

Index Terms—Functional electrical stimulation (FES), FES-cycling, repetitive learning control (RLC), switching control.

I. INTRODUCTION

REHABILITATIVE procedures and activity-based therapy have shown the potential to facilitate neurological reorganization and recovery based on the concept of motor learning by intense, repetitive task completion [1]–[3]. Robotic assistive devices and hybrid technologies, such as exoskeletons and brain–computer interfaces, have been coupled with functional electrical stimulation (FES) to provide upper and lower body training during multiple phases of rehabilitation for neurological impaired populations [4], [5]. The FES applies a potential field across muscle fibers to artificially trigger tetanic contractions [6]. Stationary FES-cycling is an often prescribed therapy to activate multiple lower limb muscles and facilitate motor learning. Furthermore, motorized assistance (i.e., adding an electric motor to the system) has been incorporated in FES-cycling studies [7], [8] to facilitate continuous, consistent exercise and thus maximize the training time to yield physiological and functional benefits [9]–[12].

Closed-loop controllers have been developed to provide robustness to the nonlinear dynamics of the cycle-rider system, including the uncertain nonlinear muscle activation dynamics [13]–[18]. FES controllers developed in [14]–[16], [19], and [20] use high-gain feedback to ensure robustness to the system's uncertainty. However, such high-frequency control methods often lead to accelerated fatigue [21], [22]. High gain feedback can yield uncomfortable stimulation intensity and amplify high-frequency aspects of the feedback signal contributing to muscle fatigue.

Switching control is inherent in FES-cycling, since multiple lower limb muscles are needed to produce a coordinated movement. Switching between multiple muscle groups is desired to achieve metabolic efficiency. In results such as [7], [13], and [23], an electric motor is included to provide assistance during regions of the crank cycle where muscle stimulation is less effective in producing torque. The goal in such results is to maximize the muscle contribution during regions of the crank cycle where efficient torque production occurs and to extend the overall exercise duration by activating the electric motor during low muscle torque output regions. Switching between multiple muscle groups and the electric motor makes the overall system a switched system. Since stability of individual subsystems does not guarantee stability of the overall system [24], additional analysis is required. For example, results such as [14] ensure stability of the overall switched system by developing reverse dwell time conditions based on known exponential convergence rates, where a sliding mode control design provides the negative-definite bound on the Lyapunov function derivative.

Motivated by the desire to reduce high-gain/high-frequency feedback, the goal in this paper is to develop an adaptive

FES-cycling controller. Due to the periodic nature of cadence tracking in cycling, the use of repetitive learning control (RLC)[1] is well motivated. However, a technical challenge to design adaptive controllers with a switching control input is that a negative-definite bound on the time derivative of the Lyapunov function candidate is unlikely without persistence of excitation.

Learning control techniques have been widely applied to systems that perform repetitive or periodic tasks, such as robotic systems. Iterative learning control (ILC) and repetitive learning control (RLC) are the two primary learning control methods. The basic premise of both control methods is to improve the tracking performance by exploiting past control signals (i.e., from previous iterations or trials) and thus compensate for an inherent state and/or time periodicity present in the system [25]–[31]. ILC addresses repetitive tracking tasks to be performed over a finite interval, where the initial conditions are set to the same value at the beginning of each trial [32], [33]. The RLC is intended for continuous operation with no resetting of the initial conditions. Lyapunov-based tools have been used to synthesize and analyze ILC, RLC, and repetitive controllers for nonlinear dynamical systems. In [34], a learning control input was designed to ensure asymptotic convergence. A saturated learning-based feedforward term was developed in [35] to compensate for periodic dynamics along with the use of adaptive control to compensate for nonperiodic dynamics. In [29], an RLC approach is constructed to track a desired trajectory with known periodicity, and with the aid of a Lyapunov–Krasovskii functional, the boundedness and convergence of the system's states are ensured. In [30], an adaptive learning method is developed using a fully saturated learning law and an iterative learning formulation to prove convergence of the states.

Many of the aforementioned learning control techniques have been implemented in FES studies due to the highly repetitive or periodic nature of the exercise. FES via ILC has been applied in trajectory following of elbow and wrist flexion [36], [37], planar and unconstrained upper arm tasks for clinical rehabilitation in stroke and multiple sclerosis populations [33], [38], [39], and foot trajectory tracking during swing phase in gait using a drop foot neuroprosthesis [40]. Similarly, the RLC has been implemented along with FES to suppress tremor by stimulating wrist flexors/extensors [41]. A single study has applied ILC for FES-cycling in computer simulation [42]. There is no previous work using one of the mentioned learning techniques in FES-cycling while involving a switching analysis between multiple muscle groups.

In this paper, an RLC is designed based on a saturated feedforward learning term developed in [35] to track a desired periodic cadence with the known period on a stationary recumbent FES-cycle. The RLC is developed to deal with the periodic tracking control problem without the need to enforce a resetting condition. A nonlinear model of the motorized cycle-rider system is used for the design of a switching controller

that activates lower limb muscles based on a predetermined activation pattern, which exploits the kinematic effectiveness of the rider, and an electric motor coupled to the drive chain. The electric motor provides the assistance as needed during the regions of the cycle crank where the muscle groups are not activated due to torque transfer inefficiencies. Experimental results on five able-bodied individuals and three participants with neurological conditions (NCs) are presented in Section V proving the feasibility of the control technique. Comparative results of two trials with and without the learning feedforward term are presented. The results indicate that the inclusion of the RLC term in the switching controller yields a lower average root-mean-squared (rms) cadence tracking error compared with the trial where the learning term was turned off. A common Lyapunov-like function is constructed by adding a Lyapunov–Krasovskii-like term to account for the periodicity of the system's desired states. Although a negative semidefinite bound is obtained on the Lyapunov derivative, as opposed to the negative-definite bound typically required for switched systems, asymptotic tracking over the time horizon of the overall switched system is ensured through the use of a corollary to the LaSalle–Yoshizawa theorem for nonsmooth systems [43, Corollary 2].

II. MODEL

A. Stationary Cycle-Rider Dynamic Model

A motorized recumbent stationary cycle and a two-legged rider can be modeled as a single degree-of-freedom (DOF) system with the following dynamics [15]:

$$M(q)\ddot{q} + V(q,\dot{q})\dot{q} + G(q) + P(q,\dot{q}) + c_d\dot{q}$$
$$= \tau_a(q,\dot{q},t) + \tau_e(t) \quad (1)$$

where $q \colon \mathbb{R}_{\geq 0} \to \mathcal{Q}$ denotes the positive clockwise measurable crank angle and $\mathcal{Q} \subseteq \mathbb{R}$ denotes the set of crank angles contained between $[0, 2\pi)$; $M \colon \mathcal{Q} \to \mathbb{R}_{>0}$, $V \colon \mathcal{Q} \times \mathbb{R} \to \mathbb{R}$, and $G \colon \mathcal{Q} \to \mathbb{R}$ denote the inertial, centripetal-Coriolis, and gravitational effects, respectively; $P \colon \mathcal{Q} \times \mathbb{R} \to \mathbb{R}$ denotes the effects of passive viscoelastic tissue forces in the rider's joints, and $c_d \in \mathbb{R}_{>0}$ is the unknown coefficient of viscous damping in the cycle; $\tau_a \colon \mathcal{Q} \times \mathbb{R} \times \mathbb{R}_{\geq 0} \to \mathbb{R}$ denotes the net active torque produced by lower limb muscle contractions of the rider, and $\tau_e \colon \mathbb{R}_{\geq 0} \to \mathbb{R}$ denotes the torque applied about the cycle crank axis by the electric motor. The full system is represented by a closed kinematic chain, thus when the orientation of a segment (i.e., crank angle) is specified for a 4-bar linkage system, the orientation of the remaining segments (e.g., knee- or hip-joint angles) is defined. Fig. 1 shows the single DOF dynamic system and the switching regions for the muscle groups and electric motor determined by the crank angle (described in Section II-B).

The passive viscoelastic effects of tissues surrounding the hip and the knee joints can be represented by [14]

$$P(q,\dot{q}) \triangleq \sum_{j \in \mathcal{J}} T_j(q) p_j(q,\dot{q})$$

where $T_j \colon \mathcal{Q} \to \mathbb{R}$ are the known joint torque transfer ratios [44] with subscript j indicating an element in the set $\mathcal{J} \triangleq \{\text{RightHip}, \text{RightKnee}, \text{LeftHip}, \text{LeftKnee}\}$ that contains
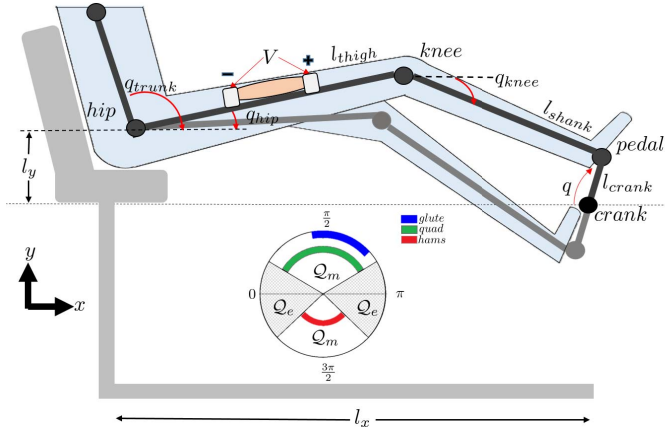

Fig. 1.   Schematic of the stationary cycle-rider system. The crank angle is denoted by q, while the knee, hip, and trunk angles are denoted by q_{knee}, q_{hip}, and q_{trunk} respectively. The thigh length, shank length, cycle crank length, and the horizontal and vertical seat positions are denoted by l_{thigh}, l_{shank}, l_{crank}, and l_x and l_y, respectively. The switching regions are depicted based on the crank angle to describe the regions of the crank cycle where the muscle groups ($\mathcal{Q}_m$) and the electric motor ($\mathcal{Q}_e$) are active. For visualization purposes in the schematic, electrical stimulation is only depicted for the right quadriceps muscle group of the rider.

right and left hip and knee joints, and $p_j: \mathcal{Q} \times \mathbb{R} \rightarrow \mathbb{R}$ denotes the torque about the rider's joint from viscoelastic tissue forces [45], [46]. The net active torque produced by a muscle contraction is

$$\tau_a(q, \dot{q}, t) \triangleq \sum_{m=1}^{\bar{M}} B_m(q, \dot{q})u_m(t) \qquad (2)$$

where $B_m: \mathcal{Q} \times \mathbb{R} \rightarrow \mathbb{R}$ represents the uncertain control effectiveness of the involved muscle groups with subscript m indicating an element in the set $\mathcal{M} \triangleq$ {RQuad, RHam, RGlute, LQuad, LHam, LGlute} that contains the right (R) and left (L) quadriceps femoris (Quad), hamstrings (Ham), and gluteal (Glute) muscle groups, respectively, where up to $\bar{M}$ muscles are contained in $\mathcal{M}$ (i.e., for this case, $\bar{M} = 6$), and $u_m: \mathbb{R}_{\geq 0} \rightarrow \mathbb{R}$ is the subsequently designed electrical stimulation intensity applied to each muscle group. The control effectiveness for each muscle group is defined as [14]

$$B_m(q, \dot{q}) \triangleq \Omega_m(q, \dot{q})T_m(q) \qquad (3)$$

for $m \in \mathcal{M}$, where $\Omega_m: \mathcal{Q} \times \mathbb{R} \rightarrow \mathbb{R}$ denotes the uncertain relationship between stimulation intensity and the muscle group's evoked force which produces a resultant torque about the joint it spans, and $T_m: \mathcal{Q} \rightarrow \mathbb{R}$ denotes the relationship between a muscle's resultant torque about a joint to torque about the crank axis. Since most muscles cross multiple joints in the lower limb, the ability of a muscle to actuate the limb in a certain direction (i.e., flexion or extension) depends on the values of T_m. Even so, there are proportional values that relate the values of T_m among muscles, which depend on muscle architecture, such as cross-sectional area, pennation angle, muscle fiber length, and flexion/extension velocity. These effects are captured in Ω_m which aids to create lower and upper bounds for the control effectiveness B_m. The following assumption is exploited in the subsequent analysis.

Assumption 1: Muscles that span multiple joints, such as the hamstrings and rectus femoris, produce torque only about the knee joint (i.e., with negligible hip coactivation). The torque output is constrained to produce torque that results in forward pedaling only based on the muscle activation switching law.

In (3), the function Ω_m is defined as [20]

$$\Omega_m(q, \dot{q}) \triangleq \zeta_m(q)\eta_m(q, \dot{q}) \cos(b_m(q)) \qquad (4)$$

where $\zeta_m: \mathcal{Q} \rightarrow \mathbb{R}$ denotes the uncertain moment arm of a muscle's output force about the joint it spans, $\eta_m: \mathcal{Q} \times \mathbb{R} \rightarrow \mathbb{R}$ denotes the nonlinear function relating the stimulation intensity to muscle force, and $b_m: \mathcal{Q} \rightarrow \mathbb{R}$ denotes the uncertain pennation angle of the muscle fibers. The following properties will be exploited in the subsequent analysis.

Property 1: The moment arm ζ_m, $\forall m \in \mathcal{M}$ is nonzero with a bounded first time derivative [47].

Property 2: The function η_m, $\forall m \in \mathcal{M}$ depends on the muscle force-length and muscle force-velocity relationships. The function η_m is bounded [48] and is positive, provided that the muscle is not fully stretched or contracting concentrically at its maximum shortening velocity [49].

Property 3: The muscle fiber pennation angle b_m, $\forall m \in \mathcal{M}$ is nonconstant [50] and bounded during muscle contractions, such that $\cos(b_m) \neq 0$ [51], [52].

Property 4: Based on Assumption 1 and Properties 1–3, Ω_m is nonzero and bounded, i.e., $c_\omega < \Omega_m < c_\Omega$, $\forall m \in \mathcal{M}$, where c_ω, $c_\Omega \in \mathbb{R}_{>0}$ are positive known constants.

The torque about the crank axis provided by the electric motor is modeled as

$$\tau_e(t) \triangleq B_e u_e(t) \qquad (5)$$

where $B_e \in \mathbb{R}_{>0}$ is a positive torque constant and $u_e: \mathbb{R}_{\geq 0} \rightarrow \mathbb{R}$ is the current applied to the electric motor.

B. Switched System Model

In this section, the rider-cycle model in (1) is further developed to account for switching between the muscle groups. The control input is commanded as stimulation intensities to the muscle groups and current to the electric motor at particular regions of the crank cycle. Stimulation is applied to each muscle group in regions of the crank cycle where the muscles can contribute to the forward pedaling motion (i.e., muscles acting as functional synergists). The electric motor is activated only in regions where the FES-induced torque is small, i.e., when the torque transfer ratios T_j, $\forall j \in \mathcal{J}$ are small. This implies that electric motor assistance is engaged during the rider's weakest torque production regions. This switching control design yields an autonomous, state-dependent, switched control system [24]. The portion of the crank cycle over which a particular muscle group is stimulated is denoted by $\mathcal{Q}_m \subset \mathcal{Q}$, $\forall m \in \mathcal{M}$, where the muscle groups are activated as described in [14]. The portions of the crank cycle over which the electric motor contributes to the torque production are denoted as $\mathcal{Q}_e \subset \mathcal{Q}$. In this development, $\mathcal{Q}_M \triangleq \cup_{m \in \mathcal{M}} \mathcal{Q}_m$ which implies that $\mathcal{Q}_e \triangleq \mathcal{Q} \backslash \mathcal{Q}_M$; that is, when no muscle group is stimulated, the electric motor is

turned on. Based on these switching laws, a piecewise constant switching signal can be developed for each muscle group, $\sigma_m \in \{0, 1\}$, and for the electric motor, $\sigma_e \in \{0, 1\}$ as

$$\sigma_m(q) \triangleq \begin{cases} 1 & \text{if } q \in \mathcal{Q}_m \\ 0 & \text{if } q \notin \mathcal{Q}_m \end{cases}, \quad \sigma_e(q) \triangleq \begin{cases} 1 & \text{if } q \in \mathcal{Q}_e \\ 0 & \text{if } q \notin \mathcal{Q}_e. \end{cases} \tag{6}$$

Fig. 1 shows the switching regions (i.e., $\mathcal{Q}_m$ and $\mathcal{Q}_e$) where the muscle groups and the electric motor are activated based on the crank angle. Using these state-dependent switching signals, the stimulation input to the muscles groups and the motor input can be defined as [13]

$$u_m(t) \triangleq k_m \sigma_m(q) v(t), \quad u_e(t) \triangleq k_e \sigma_e(q) v(t) \tag{7}$$

where $k_m, k_e \in \mathbb{R}_{>0}$, $m \in \mathcal{M}$ are positive, constant control gains, and $v \in \mathbb{R}$ is the designed control input. Substituting (7) into (1) and rearranging terms yield [13]

$$M(q)\ddot{q} + V(q, \dot{q})\dot{q} + G(q) + P(q, \dot{q}) + c_d\dot{q} = B_\sigma(q, \dot{q})v(t) \tag{8}$$

where $B_\sigma \in \mathbb{R}_{>0}$ is a lumped, switched control effectiveness term defined as

$$B_\sigma(q, \dot{q}) \triangleq \sum_{m \in \mathcal{M}} B_m(q, \dot{q})k_m\sigma_m(q) + B_e k_e \sigma_e(q). \tag{9}$$

The subscript $\sigma \in \mathcal{P} \triangleq \{1, 2, 3, \ldots N\}$ indicates the index of B_σ and switches according to the crank position. A maximum of N subsystems can be activated in a determined region of the crank cycle, i.e., the muscle groups being stimulated and the activation of the electric motor. The known sequence of switching states, which are the limit points of $\mathcal{Q}_m$, $\forall m \in \mathcal{M}$, is defined as $\{q_n\}$, $n \in \{0, 1, 2, \ldots\}$, and the corresponding sequence of unknown switching times $\{t_n\}$ is defined, such that each t_n denotes the instant when q reaches the corresponding switching state q_n. The switching signal σ is assumed to be continuous from the right [i.e., $\sigma(q) = \lim_{q \to q_n^+} \sigma(q)$]. The switched system in (8) has the following properties [13].

Property 5: $c_m \leq M \leq c_M$, where $c_m, c_M \in \mathbb{R}_{>0}$ are known constants [53].

Property 6: $|V| \leq c_V |\dot{q}|$, where $c_V \in \mathbb{R}_{>0}$ is a known constant [53].

Property 7: $|G| \leq c_G$, where $c_G \in \mathbb{R}_{>0}$ is a known constant [53].

Property 8: $|P| \leq c_{P1} + c_{P2}|\dot{q}|$, where $c_{P1}, c_{P2} \in \mathbb{R}_{>0}$ are known constants [14].

Property 9: $(1/2)\dot{M} - V = 0$ by skew symmetry [53].

Property 10: Based on Properties 1–4, the lumped switching control effectiveness is bounded as $c_b \leq B_\sigma \leq c_B$, $\forall \sigma \in \mathcal{P}$, where $c_b, c_B \in \mathbb{R}_{>0}$ are known constants.

III. Control Development

The objective is to design a controller to track a desired crank cadence. The measurable crank position trajectory tracking error $e: \mathbb{R}_{\geq 0} \to \mathbb{R}$ is defined as[2]

$$e(t) \triangleq q_d(t) - q(t) \tag{10}$$

[2]The control objective can be quantified in terms of the first time derivative of $e(t)$.

where $q_d: \mathbb{R}_{\geq 0} \to \mathbb{R}$ denotes the desired crank position with bounded time derivatives, such that $|\dot{q}_d(t)| \leq \xi_{d_1}$ and $|\ddot{q}_d(t)| \leq \xi_{d_2}$, where $\xi_{d_1}, \xi_{d_2} \in \mathbb{R}_{>0}$ are known positive constants.

Remark 1: The desired crank trajectory is periodic in the sense that $q_d(t) = q_d(t - T)$, $\dot{q}_d(t) = \dot{q}_d(t - T)$, and $\ddot{q}_d(t) = \ddot{q}_d(t - T)$ with known period T.

To facilitate the subsequent control development and stability analysis, an auxiliary tracking error $r: \mathbb{R}_{\geq 0} \to \mathbb{R}$ is defined as

$$r(t) \triangleq \dot{e}(t) + \alpha e(t) \tag{11}$$

where $\alpha \in \mathbb{R}_{>0}$ is a positive control gain. Taking the time derivative of (11) and premultiplying by M, substituting for (8) and (10), then performing some algebraic manipulation yields

$$M\dot{r} = -Vr + W_d + \chi - B_\sigma v + N_d, \tag{12}$$

where the auxiliary signals $W_d \in \mathbb{R}$, $\chi \in \mathbb{R}$, and $N_d \in \mathbb{R}$ are defined as

$$W_d \triangleq M(q_d)\ddot{q}_d + V(q_d, \dot{q}_d)\dot{q}_d + G(q_d) + c_d\dot{q}_d \tag{13}$$

$$\chi \triangleq M(q)(\ddot{q}_d + \alpha\dot{e}) + V(q, \dot{q})(\dot{q}_d + \alpha e) + G(q)$$
$$+ P(q, \dot{q}) + c_d\dot{q} - W_d - N_d \tag{14}$$

$$N_d \triangleq c_{P1} + c_{P2}\dot{q}_d. \tag{15}$$

The auxiliary signal in (15) can be upper bounded as

$$|N_d| \leq \Theta \tag{16}$$

where $\Theta \in \mathbb{R}_{>0}$ is a known positive constant. By using Properties 5–8 and (10) and (11), the mean value theorem can be used to develop an upperbound for (14) as

$$\chi \leq \rho(\|z\|)\|z\| \tag{17}$$

where $z: \mathbb{R}_{\geq 0} \to \mathbb{R}^2$ is a composite vector of error signals defined as

$$z(t) \triangleq [e(t) \, r(t)]^T \tag{18}$$

and $\rho(\cdot) \in \mathbb{R}$ is a known positive, radially unbounded, nondecreasing function. Based on (13) and the explicit boundedness of the periodic desired trajectory

$$|W_d(t)| \leq \beta_r \tag{19}$$

where $\beta_r \in \mathbb{R}$ is a known positive bounding constant. Given the open-loop error system in (12), the control input is designed as

$$v = \hat{W}_d + k_1 r + k_2\text{sgn}(r) + k_3\rho^2(\|z\|)r + k_4|\hat{W}_d|\text{sgn}(r) \tag{20}$$

where $k_1, k_2, k_3, k_4 \in \mathbb{R}_{>0}$ are control gains, $\text{sgn}(\cdot): \mathbb{R} \to [-1, 1]$ is the signum function, and $\hat{W}_d: \mathbb{R}_{\geq 0} \to \mathbb{R}$ is the repetitive control law designed as [35]

$$\hat{W}_d(t) = \text{sat}_{\beta_r}(\hat{W}_d(t - T)) + \mu r(t) \tag{21}$$

where $\mu \in \mathbb{R}_{>0}$ is a control gain and $\text{sat}_{\beta_r}(\cdot)$ is defined as

$$\text{sat}_{\beta_r}(\Xi) \triangleq \begin{cases} \Xi & \text{for } |\Xi| \leq \beta_r \\ \text{sgn}(\Xi)\beta_r & \text{for } |\Xi| > \beta_r \end{cases}$$

$\forall \Xi \in \mathbb{R}$. The closed-loop error system is obtained by substituting (20) into (12) to obtain

$$M\dot{r} = -Vr + \tilde{W}_d + \chi + N_d + \hat{W}_d - B_\sigma(\hat{W}_d + k_1 r$$
$$+ k_2 \mathrm{sgn}(r) + k_3 \rho^2(\|z\|)r + k_4 |\hat{W}_d| \mathrm{sgn}(r)) \quad (22)$$

where $\tilde{W}_d \in \mathbb{R}$ is the learning estimation error defined as $\tilde{W}_d \triangleq W_d - \hat{W}_d$. Based on the periodicity and boundedness of $W_d(t)$, $W_d(t) = \mathrm{sat}_{\beta r}(W_d(t)) = \mathrm{sat}_{\beta r}(W_d(t-T))$. Hence, by exploiting (21), the following expression can be developed for $\tilde{W}_d$:

$$\tilde{W}_d = \mathrm{sat}_{\beta r}(W_d(t-T)) - \mathrm{sat}_{\beta r}(\hat{W}_d(t-T)) - \mu r(t). \quad (23)$$

IV. STABILITY ANALYSIS

Theorem 1: The controller in (20) with the repetitive learning law in (21) ensures global asymptotic cadence tracking in the sense that

$$\lim_{t \to \infty} \dot{e}(t) = 0 \quad (24)$$

provided the control gains are selected to satisfy the following sufficient conditions:

$$\alpha > \frac{1}{2}, \quad \left(k_1 c_b + \frac{\mu}{2}\right) > \frac{1}{2}, \quad k_2 > \frac{\Theta}{c_b}, \quad k_4 > \frac{1+c_B}{c_b}$$
$$\delta = \min\left\{\left(\alpha - \frac{1}{2}\right), \left(k_1 c_b + \frac{\mu}{2} - \frac{1}{2}\right)\right\} > \frac{1}{2k_3 c_b}. \quad (25)$$

Proof: Let $V_c : \mathbb{R}^3 \times \mathbb{R}_{\geq 0} \to \mathbb{R}$ be a positive-definite, continuously differentiable function defined as

$$V_c \triangleq \frac{1}{2}e^2 + \frac{1}{2}Mr^2$$
$$+ \frac{1}{2\mu}\int_{t-T}^{t}(\mathrm{sat}_{\beta r}(W_d(\varphi)) - \mathrm{sat}_{\beta r}(\hat{W}_d(\varphi)))^2 d\varphi. \quad (26)$$

The function in (26) satisfies the following inequalities:

$$\lambda_1\|y\|^2 \leq V_c(y,t) \leq \lambda_2\|y\|^2 \quad (27)$$

where $\lambda_1 \triangleq \min((1/2), (c_m/2), (1/2\mu))$, $\lambda_2 \triangleq \max((1/2), (c_M/2), (1/2\mu))$, and $y \triangleq [z^T \ \sqrt{Q_L}]^T$, where $Q_L \triangleq \int_{t-T}^{t}(\mathrm{sat}_{\beta r}(W_d(\varphi)) - \mathrm{sat}_{\beta r}(\hat{W}_d(\varphi)))^2 d\varphi$. Let $y(t)$ be a Filippov solution to the differential inclusion $\dot{y} \in K[h](y)$, where $K[\cdot]$ is defined as [54] and h is defined by using (11) and (22) as $h \triangleq [h_1 \ h_2 \ h_3]$, where

$$h_1 \triangleq r - \alpha e$$
$$h_2 \triangleq M^{-1}\{-Vr + \tilde{W}_d + \chi + N_d - B_\sigma(k_1 r + k_2 \mathrm{sgn}(r)$$
$$+ \hat{W}_d + k_3 \rho^2(\|z\|)r + k_4 |\hat{W}_d| \mathrm{sgn}(r)) + \hat{W}_d\}$$
$$h_3 \triangleq \frac{1}{2\sqrt{Q_L}}\{(\mathrm{sat}_{\beta r}(W_d(t)) - \mathrm{sat}_{\beta r}(\hat{W}_d(t)))^2$$
$$- (\mathrm{sat}_{\beta r}(W_d(t-T)) - \mathrm{sat}_{\beta r}(\hat{W}_d(t-T)))^2\}.$$

The control input in (20) has the signum function and the discontinuous lumped control effectiveness B_σ; hence, the time derivative of (26) exists almost everywhere (a.e.), i.e., for almost all t. Based on [43, Lemma 1], $\dot{V}_c(y(t),t) \overset{a.e.}{\in} \tilde{\dot{V}}_c(y(t),t)$, where $\tilde{\dot{V}}_c$ is the generalized time derivative of (26)

along the Filippov trajectories of $\dot{y} = h(y)$ is defined as in [43] as

$$\tilde{\dot{V}}_c \triangleq \bigcap_{\xi \in \partial V_c} \xi^T K \begin{bmatrix} \dot{e} \\ \dot{r} \\ \dot{Q}_L \\ \overline{2\sqrt{Q_L}} \\ 1 \end{bmatrix} (e, r, 2\sqrt{Q_L}, t)$$

where $\partial V_c(y,t)$ is the generalized gradient of V at (y,t) defined as $\partial V_c(y,t) = \overline{\mathrm{co}}\{\lim \nabla V_c(y,t)|(y_i,t_i) \to (y,t), (y_i,t_i) \notin \Omega_{V_c}\}$, where Ω_{V_c} is the set of measure zero where the gradient of V_c is not defined and $\overline{\mathrm{co}}$ denotes convex closure [43], [55]. Since $V_c(y,t)$ is continuously differentiable in y

$$\tilde{\dot{V}}_c \overset{a.e.}{\subset} [e, \ Mr, \ \left(\frac{1}{2\mu}\right)2\sqrt{Q_L}, \ \frac{1}{2}\dot{M}r^2]K \begin{bmatrix} \dot{e} \\ \dot{r} \\ \dot{Q}_L \\ \overline{2\sqrt{Q_L}} \\ 1 \end{bmatrix}.$$

Therefore, after substituting (11) and (22), and using Property 9, the generalized time derivative of (26) can be expressed as

$$\tilde{\dot{V}}_c \overset{a.e.}{\subset} -\alpha e^2 + er + r(\tilde{W}_d + \hat{W}_d + \chi + N_d - K[B_\sigma]k_1 r$$
$$- K[B_\sigma \mathrm{sgn}(r)]k_2 - K[B_\sigma]\hat{W}_d - K[B_\sigma]k_3 \rho^2(\|z\|)r$$
$$- K[B_\sigma \mathrm{sgn}(r)]k_4|\hat{W}_d|)$$
$$- \frac{1}{2\mu}(\mathrm{sat}_{\beta r}(W_d(t-T)) - \mathrm{sat}_{\beta r}(\hat{W}_d(t-T)))^2$$
$$+ \frac{1}{2\mu}(\mathrm{sat}_{\beta r}(W_d(t)) - \mathrm{sat}_{\beta r}(\hat{W}_d(t)))^2 \quad (28)$$

where $K[B_\sigma \mathrm{sgn}(r)] = c_b SGN(r)$ such that $c_b SGN(r) = \{c_b\}$ if $r > 0$, $[-c_b, c_b]$ if $r = 0$, and $\{-c_b\}$ if $r < 0$, and $K[B_\sigma] \subset [c_b, c_B]$. Substituting for (16), (17), and (23), using Property 10, and applying Young's inequality, the expression in (28) can be upper bounded as

$$\tilde{\dot{V}}_c \overset{a.e.}{\leq} -\left(\alpha - \frac{1}{2}\right)e^2 - \left(k_1 c_b - \frac{1}{2}\right)r^2 - (k_2 c_b - \Theta)|r|$$
$$- (k_4 c_b - 1 - c_B)|\hat{W}_d||r| + \tilde{W}_d r$$
$$+ [\rho(\|z\|)\|z\||r| - k_3 c_b \rho^2(\|z\|)r^2]$$
$$- \frac{1}{2\mu}(\tilde{W}_d + \mu r)^2$$
$$+ \frac{1}{2\mu}(\mathrm{sat}_{\beta r}(W_d(t)) - \mathrm{sat}_{\beta r}(\hat{W}_d(t)))^2. \quad (29)$$

By completing the squares for the term in the bracket in (29), employing the property described in [35, Appendix I], and canceling terms, (29) can be rewritten as

$$\tilde{\dot{V}}_c \overset{a.e.}{\leq} -\left(\alpha - \frac{1}{2}\right)e^2 - \left(k_1 c_b + \frac{1}{2}\mu - \frac{1}{2}\right)r^2 + \frac{\|z\|^2}{4k_3 c_b}$$
$$- (k_2 c_b - \Theta)|r| - (k_4 c_b - 1 - c_B)|\hat{W}_d||r|. \quad (30)$$

Provided the gain conditions in (25) are satisfied, the inequality in (30) can be further upper bounded as

$$\tilde{\dot{V}}_c \overset{a.e.}{\leq} -\left(\frac{\delta}{2} - \frac{1}{4k_3 c_b}\right)\|z\|^2 - \frac{\delta}{2}\|z\|^2. \quad (31)$$

Subject	Age	Sex	Injury	Months Since Injury
A	58	M	Hemorrhagic Stroke	60
B	56	M	Ischemic Stroke	16
C	32	M	SCI C3	18

By invoking [43, Corollary 2] $|e|, |r| \to 0$ as $t \to \infty$. Since $V_c > 0$ and $\dot{V}_c \overset{a.e.}{\leq} 0$, $V_c \in \mathcal{L}_\infty$. Hence, $e(t), r(t), Q_L \in \mathcal{L}_\infty$, which implies that $y \in \mathcal{L}_\infty$. From (21), $r \in \mathcal{L}_\infty$ implies that $\hat{W}_d \in \mathcal{L}_\infty$, which along with the fact that $W_d \in \mathcal{L}_\infty$ from (19) implies that $\tilde{W}_d \in \mathcal{L}_\infty$. From the fact that $e(t), r(t) \in \mathcal{L}_\infty$ and $\hat{W}_d \in \mathcal{L}_\infty$, then $\nu \in \mathcal{L}_\infty$. Since $e(t), r(t) \in \mathcal{L}_\infty$, then $\dot{e}(t) \in \mathcal{L}_\infty$ from (11), and hence, $q(t), \dot{q}(t) \in \mathcal{L}_\infty$, which implies $\ddot{q}(t) \in \mathcal{L}_\infty$ from (8). ∎

V. EXPERIMENTS

Experiments are provided to demonstrate the performance of the controller developed in (20) with (learning ON trial) and without (learning OFF trial) the learning feedforward control term $\hat{W}_d$ in (21). The switching control input was commanded as stimulation intensities to activate a total of six lower limb muscle groups and as current to the electric motor.

A. Subjects

Five able-bodied individuals (three males and two females) with ages ranging between 21 and 25 years participated in the FES-cycling protocol at the University of Florida. Three male individuals with NCs participated in the study at Brooks Rehabilitation in Jacksonville, FL, USA. Demographics of the Brooks Rehabilitation participants are listed in Table I. Prior to participation, written informed consent was obtained from all participants, as approved by the Institutional Review Board at the University of Florida. The neurologically impaired individuals were medically stable, and a group of physical therapists was present during the study to monitor vital signs and provide assistance to the participants as needed. Both able-bodied and neurologically impaired individuals were instructed and reminded through the experiments to avoid voluntarily contributing to the pedaling task. Able-bodied individuals were not informed of the desired trajectory and could not see the desired or actual trajectory. Subject A exhibited a right-side motor impairment, sensory deficit, and aphasia (language disorder). Subject A had good muscle tone and experience with strength training exercise, but not with FES-cycling. Subject B exhibited a left-side impairment, was a part-time wheelchair user, and had previous experience with FES-cycling. Subject C is a quadriplegic due to a suffered spinal cord injury (C3 incomplete ASIA impairment scale A) with a limited range of motion for his left leg. Subject C had a previous experience with FES-induced cycling. Subjects A and B had reduced or disturbed sensitivity to electrical stimulation in the affected side. Despite the one-sided impairment demonstrated by the neurologically impaired participants, electrical stimulation was delivered to both lower extremities.
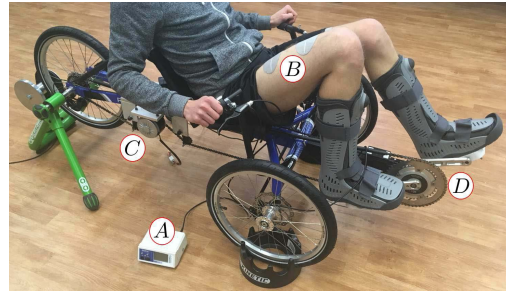

Fig. 2. Motorized FES-cycling test bed. A: current-controlled RehaStim stimulator. B: pair of PALS electrodes. C: brushed dc motor. D: cycle crank fit with sensors.

B. Experimental Setup

Testing was performed using a recumbent tricycle (TerraTrike Rover) mounted on an indoor trainer and adapted with orthotic boots, which constrained the rider's ankle to maintain the sagittal alignment of the lower legs. A brushed $24\text{-}V_{dc}$ electric motor was mounted to the frame and coupled to the drive chain. An optical encoder (US Digital) was coupled to the cycle crank to measure the crank position. The controller was implemented on a personal computer (Windows 10 OS) running a real-time target (QUARC 2.5, Quanser) via MATLAB/Simulink 2015b (MathWorks, Inc.) with a sample rate of 500 Hz. The Quanser Q8-USB data acquisition board was used to read the encoder signal and to interface with an analog motor driver (Advanced Motion Controls)[3] that commanded the current control to the electric motor. A current-controlled eight-channel stimulator (RehaStim, Hasomed GmbH) operating in Science Mode delivered biphasic, symmetric, rectangular pulses to the participant's muscle groups: quadriceps, hamstrings, and gluteal muscle groups.[4] Self-adhesive PALS electrodes ($3''$ by $5''$)[5] were placed on each muscle group in both extremities. The stimulation current amplitude was fixed at 90 mA for the quadriceps, 80 mA for the hamstrings, and 70 mA for the gluteal muscle groups.[6] The stimulation frequency was fixed at 60 Hz for all trials, and the pulsewidth was determined by u_m in (7) and commanded to the stimulator. Fig. 2 shows the motorized cycling test bed. As safety measures, participants had access to an emergency stop button and software stop conditions were implemented to limit the amount of motor current and stimulation intensity.

Electrodes were placed over the participant's muscle groups according to the electrode's manufacturer manual.[7] Initial measurements of the participant's lower extremities were recorded to obtain necessary anatomical lengths using visible landmarks as in [14]. Subjects were then seated on the tricycle,

[3]The servo drive was provided in part by the sponsorship of Advanced Motion Controls.

[4]All the healthy and neurologically impaired participants, except Subject C, were stimulated over all the six muscle groups. Subject C was stimulated only over his quadriceps and hamstrings due to time constraints and practical reasons.

[5]Surface electrodes for the study were provided compliments of Axelgaard Manufacturing Co., Ltd.

[6]All able-bodied individuals and participants with NCs have received the same current amplitudes across the lower limb muscle groups.

[7]http://www.palsclinicalsupport.com/videoElements/videoPage.php

their feet were properly placed into the orthotic pedals, and necessary seat adjustments were made to prevent knee hyperextension. The distance from the surface level to the greater trochanter and the distance from the greater trochanter to the cycle crank were measured. These measurements were used to calculate the torque transfer ratios T_m and, hence, to determine the stimulation pattern (i.e., regions of the crank cycle where the muscle groups were electrically stimulated).

For the participants with NCs, trials where the electric motor was active at low speeds were conducted to familiarize the participants with the cadence. Afterward, low intensity open-loop stimulation trains were delivered to the targeted muscle groups to assess the level of response to electrical stimulation. Cadence tracking experiments were conducted for a duration t_d between 2 and 5 min, $t_d \in [120, 300]$ s. All able-bodied individuals were able to cycle for 5 min. The desired cadence trajectory $\dot{q}_d$ smoothly approached a steady-state value of 50 revolutions per minute (RPM)[8] during a time interval of 16 s, $t \in [0, t_1]$, $t_1 = 16$. During this interval, the switching controller has only activated the motor (i.e., $\sigma_e = 1$, $q \in \mathcal{Q}_e$ for the whole crank cycle). The cadence trajectory remained constant at 50 RPM for a transition time interval of 10 s, $t \in [t_1, t_1 + 10]$, where the width of the regions of the crank cycle at which electrical stimulation is delivered (i.e., $q \in \mathcal{Q}_m$) was gradually increased until it reached a steady-state value. The width of the stimulation regions is determined by

$$\epsilon \triangleq \Lambda \max(T_m) \qquad (32)$$

where $\Lambda \in \mathbb{R}$ is a positive threshold value designed as

$$\Lambda \triangleq \begin{cases} 1.4 - \dfrac{t}{40} & \text{if } t_1 \le t < t_1 + 10 \\ 0.75 & \text{if } t \ge t_1 + 10. \end{cases} \qquad (33)$$

Both (32) and (33) define how the switching controller gradually incorporates the activation of the lower limb muscles during the experiments. This implies that the stimulation regions (i.e., regions where $\sigma_m = 1$, $q \in \mathcal{Q}_m$) grow based on whether the transfer ratios $T_m \, \forall m \in \mathcal{M}$ at every crank angle are greater than the current value of ϵ defined in (32). After the transition phase of 10 s, the stimulation regions reach a steady constant stimulation pattern (i.e., regions where T_m is greater than the 75% of the maximum value of T_m). This mechanism to smoothly integrate electrical stimulation to the switching controller was selected, because large muscle forces are needed to enable forward pedaling from rest until enough momentum has been achieved in the system. Then, the desired crank velocity $\dot{q}_d$ was designed to be a periodic function of time with an amplitude of 50 ± 5 RPM and a period of $T = 12$ s until the end of experiment, $t \in [t_1 + 10, t_d]$. This last section of the experiment where the cadence trajectory is periodic is called the steady state.

To compare the tracking performance of the RLC, two trials were developed for each enrolled participant. One trial implemented the control input designed in (20) with the

[8]For Subject C, the desired cadence trajectory $\dot{q}_d$ has approached a steady value of 40 RPM due to participant comfort.
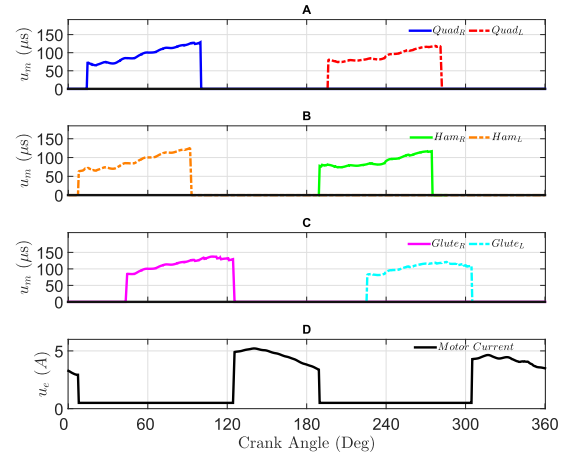

Fig. 3. FES stimulation intensities u_m and electric motor input u_e during a single crank cycle illustrating the switching controller in (7). A: Quadriceps input. B: Hamstrings input. C: Gluteal muscles input. D: Motor current input.

learning feedforward term $\hat{W}_d$ in (21) (learning ON trial). For the other trial, $\hat{W}_d = 0$, which resulted in a control input only containing the middle three terms of ν in (20) (learning OFF trial). Based on the limited availability of the participants for multiple FES-cycling sessions, especially for the population with NCs, both trials were completed in the same session. However, rest breaks were given between trials to avoid fatiguing the participant. The order of the two trials was randomized for each participant.

Fig. 3 provides an example of the switching control inputs for both the muscle stimulation intensities and the motor current distributed over a single crank cycle. The control gains introduced in (7), (11), (20), and (21) were tuned to achieve appropriate tracking performance during preliminary testing and are defined as follows: $k_m \in [0.35, 0.6]$, $k_e \triangleq 1$, $\alpha \in [2, 3]$, $k_{1,m} \in [70, 265]$, $k_{2,m} \in [5, 7.5]$, $k_{3,m} = k_{4,m} \triangleq 0.001$, $k_{1,e} \triangleq 9$, $k_{2,e} \triangleq 4$, $k_{3,e} \triangleq 0.0009$, $k_{4,e} \triangleq 0.009$, and $\mu \in [2, 32]$, where the notation $k_{\psi,\varpi}$ is used to represent the gains used for the motor control input (u_e) and the electrical stimulation input (u_m) defined in (7), where $\psi \in \{1, 2, 3, 4\}$, $\varpi \in \{m, e\}$, the subscript m denotes the muscle groups, and the subscript e is the electric motor. All the control gains were the same between the learning ON and OFF trials. However, in some OFF trials, $k_{1,m}$ was increased to achieve similar stimulation intensities for any given participant as for the ON trial.

C. Results

The FES-cycling protocol with the two trials (learning ON and OFF) was completed by all the participants. Table II summarizes the cadence rms error, the average of the cadence error $\dot{e}$, and percent error (% error) for the able-bodied individuals (S1–S5) and the participants with NCs (A–C) during steady state, $t \in [t_1 + 10, t_d]$ seconds, for both trials. The rms error was calculated over moving time interval windows of 1.2 and 12 s (corresponding to the period of the desired trajectory). Fig. 4 shows the cadence tracking performance of Subject 5 (S5), a typical result, for the learning ON trial, quantified by the rms error and the instantaneous

TABLE II

TRACKING RESULTS: rms ERROR (MOVING WINDOW OF 1.2 s), AVERAGE OF THE CADENCE ERROR $\dot{e}$, AND % ERROR REPORTED AS MEAN ±STANDARD DEVIATION (STD) DURING THE STEADY STATE OF THE EXPERIMENT FOR BOTH TRIALS WITH LEARNING (ON COLUMN) AND WITHOUT LEARNING (OFF COLUMN). STD* REPORTS THE MEAN OVER THE STANDARD DEVIATIONS

| Subject	RMS Error (RPM)		$\dot{e}$ (RPM)		% Error	
	ON	OFF	ON	OFF	ON	OFF
S1	3.31±0.53	3.94±0.56	0.04±3.34	0.03±3.98	0.03±6.82	0.05±8.07
S2	3.61±0.42	4.20±0.51	0.03±3.61	0.01±4.23	0.06±7.35	0.05±8.56
S3	4.16±0.64	4.70±0.77	0.02±4.16	0.05±4.76	0.06±8.59	0.17±9.70
S4	3.85±0.41	4.33±0.55	0.03±3.85	0.02±4.36	0.05±7.85	0.04±8.86
S5	3.45±0.49	3.81±0.39	0.03±3.47	0.01±3.83	0.03±7.09	0.02±7.78
Mean (S1-S5)	3.68	4.20	0.03	0.02	0.05	0.07
STD* (S1-S5)	0.51	0.57	3.70	4.24	7.57	8.62
A	2.14±0.45	2.85±0.40	0.01±2.19	0.01±2.92	0.02±4.33	0.02±5.82
B	4.21±1.04	4.26±1.21	0.09±4.21	0.35±4.31	0.17±8.73	0.55±8.82
C	3.15±0.63	3.37±0.72	0.02±3.23	0.01±3.42	0.00±8.06	0.11±8.72
Mean (A-C)	3.17	3.49	0.04	0.12	0.06	0.23
STD* (A-C)	0.75	0.85	3.31	3.60	7.30	7.91
Combined Mean	**3.68**	**4.09**	**0.03**	**0.06**	**0.05**	**0.12**
Combined STD*	**0.58**	**0.64**	**3.56**	**4.01**	**7.35**	**8.29**
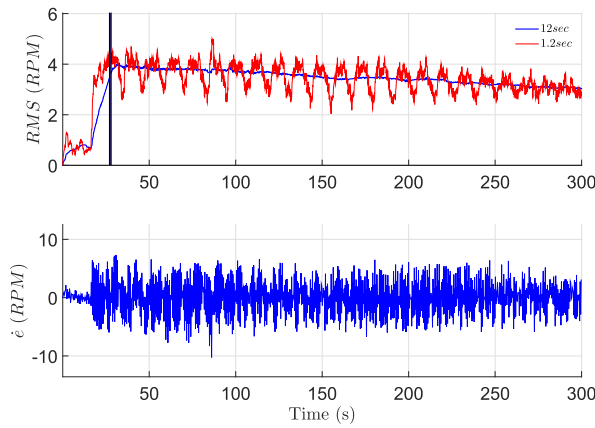
Fig. 4. Tracking performance for Subject 5 (S5) during the learning ON trial quantified by the cadence rms error (top) for two moving time interval windows and the cadence instantaneous error $\dot{e}$ (bottom). The vertical solid bar in the top plot corresponds to the time when the learning is turned ON, that is, when the steady state is reached during the trial. Instantaneous cadence is plotted by down sampling to 0.3 s.
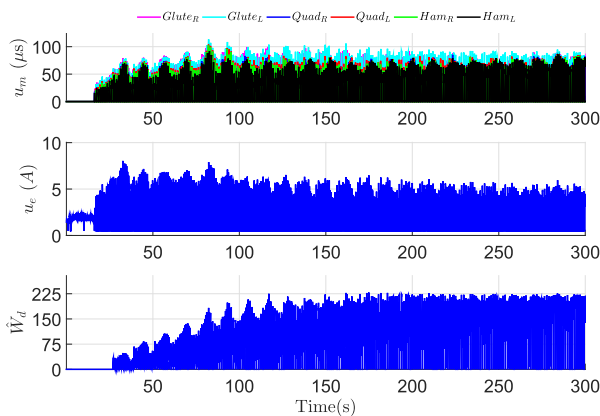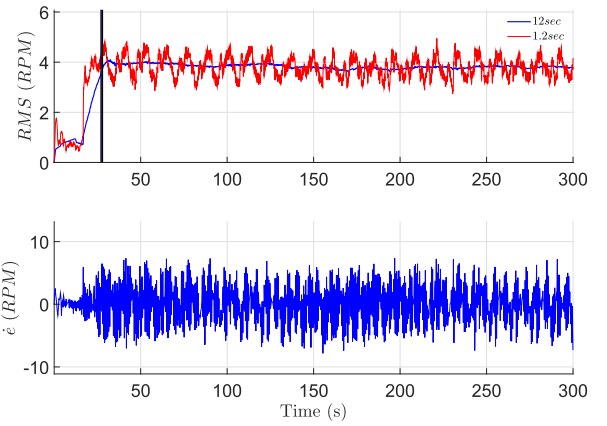

Fig. 6. Tracking performance for Subject 5 (S5) during the learning OFF trial quantified by the cadence rms error (top) for two moving time interval windows and the cadence instantaneous error $\dot{e}$ (bottom). The vertical solid bar in the top plot corresponds to the time when the learning should have been turned ON, that is, when the steady state is reached during the trial. Instantaneous cadence is plotted by down sampling to 0.3 s.

Fig. 5. Distribution of the control input to each muscle group u_m (top), the electric motor current input u_e (middle), and the learning feedforward term $\hat{W}_d$ (bottom) for Subject 5 (S5) during the learning ON trial.
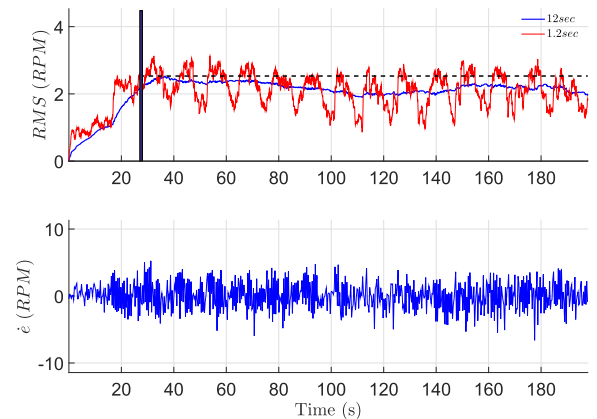

Fig. 7. Tracking performance for Subject A during the learning ON trial quantified by the cadence rms error (top) for two moving time interval windows and the cadence instantaneous error $\dot{e}$ (bottom). The vertical solid bar in the top plot corresponds to the time when the learning is turned ON, that is, when the steady state is reached during the trial. Instantaneous cadence is plotted by down sampling to 0.3 s. The dashed black line in the top plot depicts the maximum rms error for the moving 12-s window.

error $\dot{e}$. Fig. 5 shows the stimulation intensities u_m delivered to the muscle groups, the electric motor current input u_e, and the learning feedforward term $\hat{W}_d$ for Subject 5 (S5) for the learning ON trial.

Fig. 6 shows the tracking performance of Subject 5 (S5) for the learning OFF trial. As an example of the tracking of the participants with NCs, Fig. 7 shows the tracking performance
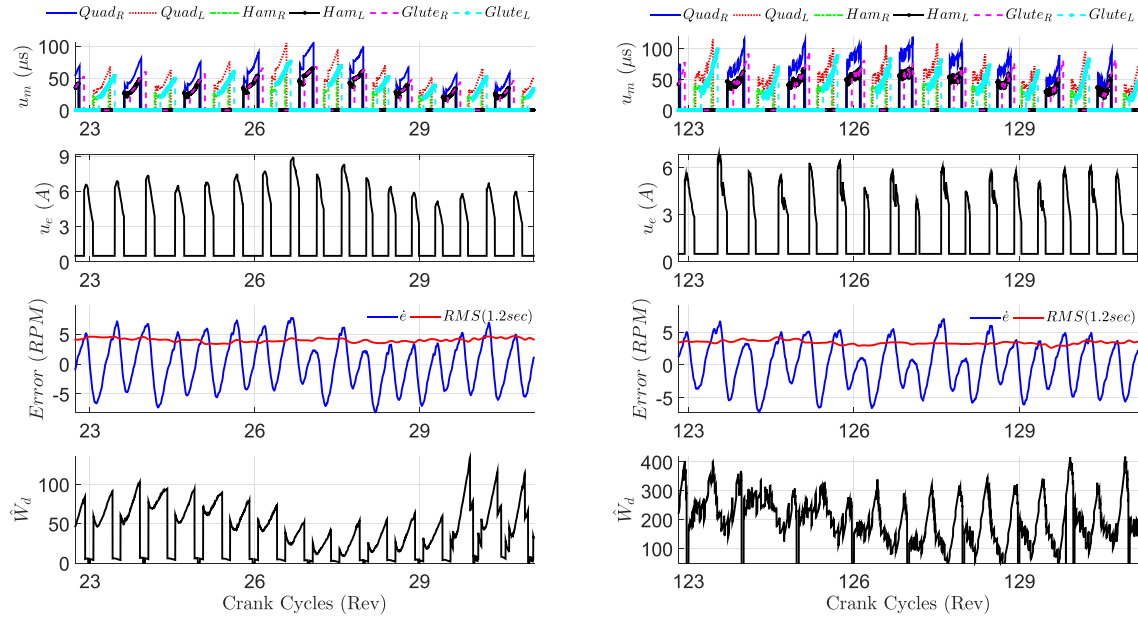
Fig. 8. FES control inputs u_m, motor current input u_e, cadence tracking error (rms and instantaneous error $\dot{e}$), and learning-based feedforward term $\hat{W}_d$ during several consecutive crank cycles at the beginning of the learning ON trial (left column) and 100 crank cycles later in the same trial (right column) for Subject 2 (S2).

of Subject A during the learning ON trial. Fig. 8 shows the muscle intensities delivered to all the muscle groups, the motor current input, the cadence tracking errors (rms and instantaneous cadence tracking error $\dot{e}$), and the learning-based feedforward term $\hat{W}_d$ during several consecutive crank cycles at the beginning of the ON trial and then 100 crank cycles later for Subject 2 (S2).

D. Statistical Analysis

A Wilcoxon signed ranked test was performed at a significance level of $\alpha = 0.05$ to test for statistically significant differences between the rms cadence tracking error between trials (learning ON versus learning OFF) for the total number of participants ($N = 8$). For both able-bodied and participants with NCs, the learning ON trial yielded a lower rms cadence error than the learning OFF trial ($p - value = 0.0156$) with the median values of 3.61 and 4.20, respectively.

E. Discussion

The experimental results demonstrate the feasibility of the controller in (20) to track a desired cadence with the combined contribution of FES activation of the lower limb muscles and motor assistance. The inclusion of the learning-based feedforward term designed in (21) during the ON trial resulted in lower rms cadence error and instantaneous tracking error $\dot{e}$ compared with the OFF trial, where the learning term was neglected for both able-bodied individuals and participants with NCs. The mean instantaneous cadence tracking error is 0.03 ± 3.70 RPM for the ON trial and 0.02 ± 4.24 RPM for the OFF trial across all healthy individuals. For people with NCs, the mean instantaneous cadence tracking error is 0.04 ± 3.31 RPM for the ON trial and 0.12 ± 3.60 RPM for the OFF trial.

Implementation of the RLC offers the advantage of adding a feedforward term to the control input by exploiting the system's periodic desired trajectories rather than using a model-based control, such as in classical adaptive control where a regression matrix has to be known. In other words, the RLC is added to a robust controller aiming to improve the tracking performance, as shown in Section V-C.

Despite the fact that the stability analysis yields an asymptotic tracking result, there are factors in the experiment that could affect the steady-state tracking error, such as the inherent electromechanical delay that occurs between the input being delivered to the muscle and actual force production [56] or the effect of nonperiodic disturbances such as muscle fatigue. Additional challenges were encountered while conducting experiments with participants possessing NCs such as observed intermittent muscle spasms, asymmetries between the lower extremities, and potential electrical stimulation sensitivity from residual sensory feedback. These challenges have resulted in shorter experiment durations (e.g., $t_d < 300$ s) for the participants with NCs compared with able-bodied individuals. Although Subjects A and B had a residual motor control on their affected side and full motor control in their contralateral side, no voluntary contribution to the pedaling task was provided (monitored by the consistent nonvanishing stimulation intensities delivered throughout the experiment) to compare their tracking performance with Subject C, who had no neurological motor control. The results reported in Table II are representative of typical performance during FES-cycling tasks.

The results show that by switching the control effort between muscle activation via FES and the electric motor, the participants with NCs were capable of producing smooth cadence without any voluntary contribution. This relevant

observation demonstrates the efficacy of the control technique, since it has been reported that the intact leg of subjects with hemiparesis provides enough muscle force without FES (i.e., voluntary contribution only) to complete the pedaling task and to compensate for the affected leg [57], [58]. However, this inherent compensation by the healthy leg diminishes the potential FES benefits during cycling. Moreover, in [57], 90% of the stroke participants were unable to increase crank contribution when receiving open-loop stimulation on their affected limb. In [58], a posttraining voluntary pedaling test was conducted where FES was also delivered open loop to both the affected and intact lower limbs of participants with postacute hemiparesis which showed improved motion symmetry and activation timing of the impaired muscles. For spinal cord injured populations, power output, metabolic rate, and muscle strength are increased after FES-cycling training using fixed stimulation parameters [59]. Clinical trials with larger neurologically impaired populations are required to investigate the impact of the control method developed in this paper. Ultimately, a cycling protocol that adopts closed-loop FES and learning control for the affected limb and motivates voluntary intent for the intact limb, while using a split crank cycle may result in a more suitable rehabilitation approach for people with stroke.

VI. CONCLUSION

A switched controller with a learning-based feedforward term was designed to activate the lower limb muscles and an electric motor to yield asymptotic cadence tracking. The switching signal commands stimulation intensities to the muscle groups when they can contribute efficiently to the pedaling task and activates the electric motor in regions of the crank cycle where muscles have low torque efficiency. The developed controller compensates for periodic dynamics (based on the desired periodic reference trajectory) using a repetitive learning feedforward term combined with robust feedback terms. Global asymptotic tracking is achieved with the aid of a corollary to the LaSalle–Yoshizawa theorem for nonsmooth systems in [43].

The RLC was successfully tested in experiments conducted on five able-bodied individuals and three participants with NCs. The added value of the RLC (e.g., against a pure robust controller) for cadence tracking was illustrated by comparing the tracking performance during two trials with and without learning (ON and OFF trials, respectively). For the healthy control group, a mean rms cadence error of 3.68±0.51 RPM (0.05±7.57% error) was obtained for the ON trial compared to the rms cadence error of 4.20±0.57 RPM (0.07±8.62% error) for the OFF trial. For the patient population, a mean rms cadence error of 3.17 ± 0.75 RPM ($0.06 \pm 7.30\%$ error) was obtained for the ON trial compared with the rms cadence error of 3.49 ± 0.85 RPM ($0.23 \pm 7.91\%$ error) for the OFF trial. The results on the participants with NCs demonstrate the ability to yield repetitive cycling despite lower limb motion asymmetries, sensitivity to electrical stimulation, constrained range of motion, and lack of neurological motor control (dysfunction to coordinate muscles and limbs to achieve a

motor skill). The developed controller holds the potential to be extended to a larger set of populations with NCs, such as Parkinson's disease, traumatic brain injury, cerebral palsy, and multiple sclerosis. Additional challenges that may arise through the testing of a broader population includes muscle atrophy (limited muscle mass and tone) that may lead to a mitigated response to applied electrical stimuli. Moreover, learning control techniques can be applied for different tracking objectives in FES-based exercise such as power control (i.e., track a desired torque output). To advance the impact of this system for rehabilitation, an extension of the developed control technique to the case where the participants are allowed and encouraged to participate in cycling performance is the focus of future research. Future work also includes the long-term investigation of the rehabilitative benefits of FES-cycling using learning control methods in clinical trials.

REFERENCES

[1] V. R. Edgerton *et al.*, "Retraining the injured spinal cord," *J. Physiol.*, vol. 533, no. 1, pp. 15–22, 2001.

[2] V. R. Edgerton and R. R. Roy, "Paralysis recovery in humans and model systems," *Current Opinion Neurobiol.*, vol. 12, no. 6, pp. 658–667, 2002.

[3] M. L. Jones *et al.*, "Activity-based therapy for recovery of walking in individuals with chronic spinal cord injury: Results from a randomized clinical trial," *Arch. Phys. Med. Rehabil.*, vol. 95, no. 12, pp. 2239–2246, 2014.

[4] A. J. del Ama, Á. Gil-Agudo, J. L. Pons, and J. C. Moreno, "Hybrid FES-robot cooperative control of ambulatory gait rehabilitation exoskeleton," *J. Neuroeng. Rehabil.*, vol. 11, no. 1, p. 27, 2014.

[5] J.-M. Belda-Lois *et al.*, "Rehabilitation of gait after stroke: A review towards a top-down approach," *J. Neuroeng. Rehabil.*, vol. 8, p. 66, Dec. 2011.

[6] P. H. Peckham and J. S. Knutson, "Functional electrical stimulation for neuromuscular applications," *Annu. Rev. Biomed. Eng.*, vol. 7, pp. 327–360, Mar. 2005.

[7] K. J. Hunt *et al.*, "Control strategies for integration of electric motor assist and functional electrical stimulation in paraplegic cycling: Utility for exercise testing and mobile cycling," *IEEE Trans. Neural Syst. Rehabil. Eng.*, vol. 12, no. 1, pp. 89–101, Mar. 2004.

[8] E. Ambrosini, S. Ferrante, T. Schauer, G. Ferrigno, F. Molteni, and A. Pedrocchi, "Design of a symmetry controller for cycling induced by electrical stimulation: Preliminary results on post-acute stroke patients," *Artif. Organs*, vol. 34, no. 8, pp. 663–667, 2010.

[9] S. Ferrante, A. Pedrocchi, G. Ferrigno, and F. Molteni, "Cycling induced by functional electrical stimulation improves the muscular strength and the motor control of individuals with post-acute stroke," *Eur. J. Phys. Rehabil. Med.*, vol. 44, no. 2, pp. 159–167, 2008.

[10] L. Griffin *et al.*, "Functional electrical stimulation cycling improves body composition, metabolic and neural factors in persons with spinal cord injury," *J. Electromyogr. Kinesiol.*, vol. 19, no. 4, pp. 614–622, 2009.

[11] H. R. Berry *et al.*, "Cardiorespiratory and power adaptation to stimulated cycle training in paraplegia," *Med. Sci. Sports Exerc.*, vol. 40, no. 9, pp. 1573–1580, Sep. 2008.

[12] C.-W. Peng *et al.*, "Review: Clinical benefits of functional electrical stimulation cycling exercise for subjects with central neurological impairments," *J. Med. Biol. Eng.*, vol. 31, no. 1, pp. 1–11, 2011.

[13] M. J. Bellman, R. J. Downey, A. Parikh, and W. E. Dixon, "Automatic control of cycling induced by functional electrical stimulation with electric motor assistance," *IEEE Trans. Autom. Sci. Eng.*, vol. 14, no. 2, pp. 1225–1234, Apr. 2017.

[14] M. J. Bellman, T.-H. Cheng, R. J. Downey, C. J. Hass, and W. E. Dixon, "Switched control of cadence during stationary cycling induced by functional electrical stimulation," *IEEE Trans. Neural Syst. Rehabil. Eng.*, vol. 24, no. 12, pp. 1373–1383, Dec. 2016.

[15] M. J. Bellman, T.-H. Cheng, R. J. Downey, and W. E. Dixon, "Stationary cycling induced by switched functional electrical stimulation control," in *Proc. Amer. Control Conf.*, Jun. 2014, pp. 4802–4809.

[16] M. J. Bellman, T.-H. Cheng, R. Downey, and W. E. Dixon, "Cadence control of stationary cycling induced by switched functional electrical stimulation control," in *Proc. IEEE Annu. Conf. Decis. Control*, Dec. 2014, pp. 6260–6265.

[17] W. E. Dixon and M. Bellman, "Cycling induced by functional electrical stimulation: A control systems perspective," *ASME Dyn. Syst. Control Mag.*, vol. 4, no. 3, pp. 3–7, Sep. 2016.

[18] A. Farhoud and A. Erfanian, "Fully automatic control of paraplegic FES pedaling using higher-order sliding mode and fuzzy logic control," *IEEE Trans. Neural Syst. Rehabil. Eng.*, vol. 22, no. 3, pp. 533–542, May 2014.

[19] R. J. Downey, T.-H. Cheng, M. J. Bellman, and W. E. Dixon, "Closed-loop asynchronous neuromuscular electrical stimulation prolongs functional movements in the lower body," *IEEE Trans. Neural Syst. Rehabil. Eng.*, vol. 23, no. 6, pp. 1117–1127, Nov. 2015.

[20] N. Sharma, K. Stegath, C. M. Gregory, and W. E. Dixon, "Nonlinear neuromuscular electrical stimulation tracking control of a human limb," *IEEE Trans. Neural Syst. Rehabil. Eng.*, vol. 17, no. 6, pp. 576–584, Dec. 2009.

[21] C. M. Gregory, W. E. Dixon, and C. S. Bickel, "Impact of varying pulse frequency and duration on muscle torque production and fatigue," *Muscle Nerve*, vol. 35, no. 4, pp. 504–509, Apr. 2007. [Online]. Available: http://ncr.mae.ufl.edu/papers/muscle07.pdf

[22] S. A. Binder-Macleod, E. E. Halden, and K. A. Jungles, "Effects of stimulation intensity on the physiological responses of human motor units," *Med. Sci. Sports. Exerc.*, vol. 27, no. 4, pp. 556–565, Apr. 1995.

[23] J. Szecsi, A. Straube, and C. Fornusek, "Comparison of the pedalling performance induced by magnetic and electrical stimulation cycle ergometry in able-bodied subjects," *Med. Eng. Phys.*, vol. 36, no. 4, pp. 484–489, 2014.

[24] D. Liberzon, *Switching in Systems and Control*. Boston, MA, USA: Birkhäuser, 2003.

[25] S. Arimoto, S. Kawamura, and F. Miyazaki, "Bettering operation of dynamic systems by learning: A new control theory for servomechanism or mechatronics systems," in *Proc. IEEE Conf. Decis. Control*, Dec. 1984, pp. 1064–1069.

[26] R. H. Middleton, G. C. Goodwin, and R. W. Longman, "A method for improving the dynamic accuracy of a robot performing a repetitive task," *Int. J. Robot. Res.*, vol. 8, no. 5, pp. 67–74, Oct. 1989.

[27] Y. Wang, F. Gao, and F. J. Doyle, "Survey on iterative learning control, repetitive control, and run-to-run control," *J. Process Control*, vol. 19, no. 10, pp. 1589–1600, Dec. 2009.

[28] H.-S. Ahn, K. L. Moore, and Y. Chen, *Iterative Learning Control: Robustness and Monotonic Convergence for Interval Systems*, E. Sontag, M. Thoma, A. Isidori, and J. van Schuppen, Eds. London, U.K.: Springer-Verlag, 2007.

[29] J.-X. Xu and R. Yan, "On repetitive learning control for periodic tracking tasks," *IEEE Trans. Autom. Control*, vol. 51, no. 11, pp. 1842–1848, Nov. 2006.

[30] M. Sun, S. S. Ge, and I. M. Y. Mareels, "Adaptive repetitive learning control of robotic manipulators without the requirement for initial repositioning," *IEEE Trans. Robot.*, vol. 22, no. 3, pp. 563–568, Jun. 2006.

[31] M. Yu, X. Ye, and D. Qi, "Repetitive learning control for triangular systems with unknown control directions," *IET Control Theory Appl.*, vol. 5, no. 17, pp. 2045–2051, 2011.

[32] D. A. Bristow, M. Tharayil, and A. G. Alleyne, "A survey of iterative learning control: A learning-based method for high performance tracking control," *IEEE Control Syst. Mag.*, vol. 26, no. 3, pp. 96–114, Jun. 2006.

[33] C. T. Freeman, E. Rogers, J. H. Burridge, A.-M. Hughes, and K. L. Meadmore, *Iterative Learning Control for Electrical Stimulation and Stroke Rehabilitation* (SpringerBriefs in Control, Automation and Robotics), 1st ed. London, U.K.: Springer-Verlag, 2015.

[34] W. Messner, R. Horowitz, W.-W. Kao, and M. Boals, "A new adaptive learning rule," *IEEE Trans. Autom. Control*, vol. 36, no. 2, pp. 188–197, Feb. 1991.

[35] W. E. Dixon, E. Zergeroglu, D. M. Dawson, and B. T. Costic, "Repetitive learning control: A Lyapunov-based approach," *IEEE Trans. Syst., Man, Cybern. B, Cybern.*, vol. 32, no. 4, pp. 538–545, Aug. 2002.

[36] H. Wu, Z. Zhou, S. Xiong, and W. Zhang, "Adaptive iteration learning control and its applications for FNS multi-joint motion," in *Proc. IEEE Instrum. Meas. Technol. Conf. (IMTC)*, May 2000, pp. 983–987.

[37] H. Dou, K. K. Tan, T. H. Lee, and Z. Zhou, "Iterative learning feedback control of human limbs via functional electrical stimulation," *Control Eng. Pract.*, vol. 7, no. 3, pp. 315–325, 1999.

[38] C. T. Freeman, E. Rogers, A.-M. Hughes, J. H. Burridge, and K. L. Meadmore, "Iterative learning control in health care: Electrical stimulation and robotic-assisted upper-limb stroke rehabilitation," *IEEE Control Syst.*, vol. 32, no. 1, pp. 18–43, Feb. 2012.

[39] P. Sampson *et al.*, "Using functional electrical stimulation mediated by iterative learning control and robotics to improve arm movement for people with multiple sclerosis," *IEEE Trans. Neural Syst. Rehabil. Eng.*, vol. 24, no. 2, pp. 235–248, Feb. 2016.

[40] T. Seel, C. Werner, J. Raisch, and T. Schauer, "Iterative learning control of a drop foot neuroprosthesis—Generating physiological foot motion in paretic gait by automatic feedback control," *Control Eng. Pract.*, vol. 48, pp. 87–97, Mar. 2016.

[41] C. T. Freeman, P. Sampson, J. H. Burridge, and A.-M. Hughes, "Repetitive control of functional electrical stimulation for induced tremor suppression," *Mechatronics*, vol. 32, pp. 79–87, Dec. 2015.

[42] K.-M. Wang, T. Schauer, H. Nahrstaedt, and J. Raisch, "Iterative learning control of cadence for functional electrical stimulation induced cycling in paraplegia," in *Proc. Conf. Int. Funct. Electr. Stimulation Soc.*, Sep. 2009, pp. 71–73.

[43] N. Fischer, R. Kamalapurkar, and W. E. Dixon, "LaSalle-Yoshizawa corollaries for nonsmooth systems," *IEEE Trans. Autom. Control*, vol. 58, no. 9, pp. 2333–2338, Sep. 2013.

[44] E. S. Idsø, T. A. Johansen, and K. J. Hunt, "Finding the metabolically optimal stimulation pattern for FES-cycling," in *Proc. Conf. Int. Funct. Electr. Stimulation Soc.*, Bournemouth, U.K., Sep. 2004, pp. 1–3.

[45] T. Schauer *et al.*, "Online identification and nonlinear control of the electrically stimulated quadriceps muscle," *Control Eng. Pract.*, vol. 13, no. 9, pp. 1207–1219, Sep. 2005.

[46] M. Ferrarin and A. Pedotti, "The relationship between electrical stimulus and joint torque: A dynamic model," *IEEE Trans. Rehabil. Eng.*, vol. 8, no. 3, pp. 342–352, Sep. 2000.

[47] J. L. Krevolin, M. G. Pandy, and J. C. Pearce, "Moment arm of the patellar tendon in the human knee," *J. Biomech.*, vol. 37, no. 5, pp. 785–788, 2004.

[48] T. Watanabe, R. Futami, N. Hoshimiya, and Y. Handa, "An approach to a muscle model with a stimulus frequency-force relationship for FES applications," *IEEE Trans. Rehabil. Eng.*, vol. 7, no. 1, pp. 12–18, Mar. 1999.

[49] E. P. Widmaier, H. Raff, and K. T. Strang, *Human Physiology: The Mechanisms of Body Function*, 9th ed. New York, NY, USA: McGraw-Hill, 2004.

[50] T. S. Buchanan, D. G. Lloyd, K. Manal, and T. F. Besier, "Neuromusculoskeletal modeling: Estimation of muscle forces and joint moments and movements from measurements of neural command," *J. Appl. Biomech.*, vol. 20, no. 4, pp. 367–395, 2004.

[51] R. L. Lieber and J. Fridén, "Functional and clinical significance of skeletal muscle architecture," *Muscle Nerve*, vol. 23, no. 11, pp. 1647–1666, Nov. 2000.

[52] O. M. Rutherford and D. A. Jones, "Measurement of fibre pennation using ultrasound in the human quadriceps *in vivo*," *Eur. J. Appl. Physiol. Occupat. Physiol.*, vol. 65, pp. 433–437, Nov. 1992.

[53] W. E. Dixon, A. Behal, D. M. Dawson, and S. P. Nagarkatti, *Nonlinear Control of Engineering Systems: A Lyapunov-Based Approach*. Boston, MA, USA: Springer, 2003.

[54] A. F. Filippov, "Differential equations with discontinuous right-hand side," *Amer. Math. Soc. Transl.*, vol. 42, no. 2, pp. 199–231, 1964.

[55] F. H. Clarke, *Optimization and Nonsmooth Analysis*. Reading, MA, USA: Addison-Wesley, 1983.

[56] R. J. Downey, M. Merad, E. J. Gonzalez, and W. E. Dixon, "The time-varying nature of electromechanical delay and muscle control effectiveness in response to stimulation-induced fatigue," *IEEE Trans. Neural Syst. Rehabil. Eng.*, vol. 25, no. 9, pp. 1397–1408, Sep. 2017.

[57] J. Szecsi, C. Krewer, F. Müller, and A. Straube, "Functional electrical stimulation assisted cycling of patients with subacute stroke: Kinetic and kinematic analysis," *Clin. Biomech.*, vol. 23, no. 8, pp. 1086–1094, Oct. 2008.

[58] E. Ambrosini, S. Ferrante, G. Ferrigno, F. Molteni, and A. Pedrocchi, "Cycling induced by electrical stimulation improves muscle activation and symmetry during pedaling in hemiparetic patients," *IEEE Trans. Neural Syst. Rehabil. Eng.*, vol. 20, no. 3, pp. 320–330, May 2012.

[59] T. W. J. Janssen and D. D. Pringle, "Effects of modified electrical stimulation-induced leg cycle ergometer training for individuals with spinal cord injury," *J. Rehabil. Res. Develop.*, vol. 45, no. 6, pp. 819–830, 2008.

Victor H. Duenas received the B.S. degree from the University of Texas at El Paso, El Paso, TX, USA, in 2014, and M.S. degree in mechanical engineering from the University of Florida, Gainesville, FL, USA, in 2016, where he is currently pursuing the Ph.D. degree in mechanical engineering under the supervision of Dr. W. Dixon.

His current research interests include nonlinear and adaptive control for rehabilitation robotics, neuromuscular control, and switched systems.

Christian A. Cousin received the bachelor's and master's degrees in mechanical engineering with a minor in electrical engineering and mathematics from the University of Florida, Gainesville, FL, USA, where he is currently pursuing the Ph.D. degree in mechanical engineering with a focus on Lyapunov-based switched systems analysis involving nonlinear human–machine interaction using functional electrical stimulation and robots to aid in the rehabilitation of the extremities.

He has been with the Nonlinear Controls and Robotics Group, University of Florida, since 2015.

Mr. Cousin is a National Science Foundation Graduate Research Fellow.

Anup Parikh received the B.S. degree in mechanical and aerospace engineering, the M.S. degree in mechanical engineering, and the Ph.D. degree in aerospace engineering from the University of Florida, Gainesville, FL, USA.

He is currently a Post-Doctoral Researcher with Sandia National Laboratories, Albuquerque, NM, USA. His current research interests include Lyapunov-based estimation and control theory, machine vision, and autonomous systems.

Paul Freeborn received the B.S. degree in exercise physiology from Jacksonville University, Jacksonville, FL, USA, in 2014.

He is currently a Center Coordinator with the Brooks Rehabilitation Motion Analysis Center, Jacksonville, FL, USA. His current research interests include the area of functional electrical stimulation and the use of technology in rehabilitation.

Emily J. Fox received the D.P.T degree from the University of St. Augustine, St. Augustine, FL, USA, and the Ph.D. degree from the University of Florida, Gainesville, FL, USA.

She is currently a Research Assistant Professor with the Department of Physical Therapy, University of Florida, Gainesville, FL, USA, and a Clinical Research Scientist with the Brooks Rehabilitation Clinical Research Center, Jacksonville, FL, USA. She is also the Director of the Brooks Rehabilitation Motion Analysis Center, Jacksonville, FL, USA. Her current research interests include neuromuscular control and functional recovery following neurologic injury or disease, and also the development and investigation of innovative approaches, such as electrical stimulation to enhance motor function and recovery.

Dr. Fox is a Neurologic Clinical Specialist.

Warren E. Dixon (M'94–F'16) received the Ph.D. degree from the Department of Electrical and Computer Engineering, Clemson University, Clemson, SC, USA, in 2000.

He was a Research Staff Member and a Eugene P. Wigner Fellow with the Oak Ridge National Laboratory, Oak Ridge, TN, USA, until 2004. He joined the Mechanical and Aerospace Engineering Department, University of Florida, Gainesville, FL, USA, as an Ebaugh Professor. His current research interests include the development and application of Lyapunov-based control techniques for uncertain nonlinear systems.

Dr. Dixon is an ASME Fellow. He received the 2015 and 2009 American Automatic Control Council O. Hugo Schuck (Best Paper) Award, the 2013 Fred Ellersick Award for the Best Overall MILCOM Paper, the 2011 American Society of Mechanical Engineers Dynamics Systems and Control Division Outstanding Young Investigator Award, the 2006 IEEE Robotics and Automation Society Early Academic Career Award, and the NSF CAREER Award (2006–2011).